

Graphene Langmuir-Schaefer films Decorated by Pd Nanoparticles for NO₂ and H₂ Gas Sensors

Dmytro Kostiuk, Stefan Luby, Peter Siffalovic, Monika Benkovicova, Jan Ivanco, Matej Jergel, Eva Majkova

Institute of Physics, Slovak Academy of Sciences, Dubravská cesta 9, 84511, Bratislava, Slovakia, stefan.luby@savba.sk

NO₂ and H₂ gas sensing by few-layer graphene (FLG) were studied in dependence on the annealing and decoration of graphene by palladium nanoparticles (NPs). Graphene was deposited onto SiO₂ (500 nm)/Si substrates by a modified Langmuir-Schaefer technique. A solution of FLG flakes in 1-methyl-2-pyrrolidone was obtained by a mild sonication of the expanded milled graphite. FLG films were characterized by atomic force microscopy, X-ray diffraction, Raman spectroscopy, and the Brunauer-Emmett-Teller method. Average FLG flake thickness and lateral dimension were 5 nm and 300 nm, respectively. Drop casting of Pd NP (6–7 nm) solution onto FLG film was applied to decorate graphene by Pd. The room temperature (RT) resistance of the samples was stabilized at 15 kΩ by vacuum annealing. Heating cycles of FLG film revealed its semiconducting character. The gas sensing was tested in the mixtures of dry air with H₂ gas (10 to 10 000 ppm) and NO₂ gas (2 to 200 ppm) between RT and 200 °C. The response of 26 % to H₂ was achieved by FLG with Pd decoration at 70 °C and 10 000 ppm of H₂ in the mixture. Pure FLG film did not show any response to H₂. The response of FLG with Pd to 6 ppm of NO₂ at RT was ≥ 23 %. It is 2 times larger than that of the pure FLG sample. Long term stability of sensors was studied.

Keywords: Few-layer graphene, Pd nanoparticles, gas sensors, NO₂ and H₂ sensing.

1. INTRODUCTION

Since 60-ties of the 20th century metal oxides have been the main pillar of solid-state sensors of gases and vapors [1]. However, immediately after graphene appeared at the stage, it has been extensively studied and reviewed [2]-[6] in terms of gas sensor material owing to its combination of large surface area (theoretically 2 630 m²/g), high carrier mobility, thermal conductivity, strength, Young modulus, and flexibility [4], [6]. Graphene 2D inorganic analogues like MoS₂, WS₂, WSe₂, etc., attracted attention in gas sensing down to ppb range too [6]-[8]. Yet the strong graphene sp² bonds are the cause of low chemical reactivity [3] since intrinsic graphene has no dangling bonds required for gas/vapor surface adsorption [2], [3], [5]. Adsorption energies of various gases on graphene [4] are very low – in the range of hundredths of eV (e.g., of 0.067 eV for NO₂). Thereby adsorption and, consequently, the sensitivity of sensors could be increased by patterning of graphene [4], [9], by its chemical doping or functionalization/decoration by metal nanoparticles (NPs) such as Pt, Pd, Au [4], [10]-[12], or by UV irradiation in ozone [13]. Nevertheless, the low reactivity of graphene is compensated by low electrical noise; therefore, very small amounts of gas adsorbed on graphene, even a single molecule, could be detected [14].

The major advantage of graphene-based sensors over the metal oxide ones is markedly lower operating temperature ranging down to even room temperature (RT) [6] required in explosive environments. The low working voltage of graphene sensors provides better integrability into electronic circuits. The study of gas reactions on the surface of graphene and its electrical conductivity as a by-product of sensor research is a source of knowledge about the material [14].

The results mentioned above were often obtained with chemical vapor deposited graphene [13] which does not belong to cheap materials. Preparation of graphene nanoflakes by liquid exfoliation of expanded graphite introduced by Hernandez et al. [15] is a step toward the decrease of the production costs. The resulting few-layer graphene (FLG) is prepared in various solvents. IUPAC defines it as a material composed of 3 to 10 monolayers [16]. For the preparation of a continuous layer (a nanofilm) from the FLG colloidal solution the Langmuir-Blodgett deposition is often used (e.g., [17]). Among the FLG applications in sensors we may mention detection of CO₂ and LPG by 3 – 4 monolayers thick [16] or NO₂ by 7 – 10 monolayers thick FLG [18].

In this paper we report on low priced FLG nanostructured sensors based on graphene flakes decorated by Pd NPs. Our previous results on H₂ sensors [19] are extended here by NO₂

sensing with the aim to compare the surface reactions of both reducing and oxidizing gas and to check the FLG conductivity type. The NO₂ sensing by graphene and metal oxide sensors [20] is compared here as well.

2. EXPERIMENTAL DETAILS

FLG solution was obtained by the liquid-phase exfoliation technique [15]. Commercially available expanded milled graphite [21] (SGL-Carbon, Germany) was used. After 1 min of microwave irradiation at 800 W it was sonicated 60 min at 200 W. 1-methyl-2-pyrrolidone was used as solvent. Initial concentration of graphite in solution was 10 mg/ml. Centrifugation at 10⁴g/10 min followed after overnight sedimentation. The resulting material with the concentration of 0.2 mg/ml was collected and kept 1 month in room conditions to allow the sedimentation of big particles.

FLG films were deposited onto SiO₂ (500 nm)/Si substrates by a modified Langmuir-Schaefer technique (LS) [22]. Here the substrate is submerged under the water pumped slowly from the trough while FLG sinks down onto the substrate. Then continuous arrays could be created. Prior to the deposition the substrates were irradiated by UV ($\lambda = 254$ nm/15 min) to improve their hydrophilic character (the contact angle decreased from 45° to 10°). The substrates were fixed in a sample holder with an angle around 5° with respect to the air/water interface. The FLG solution was dropped onto the interface in the high compression trough. The consecutive phases of the FLG LS film formation at the air-water interface monitored by the long focal length optical microscope are shown in Fig.1. At the beginning of the compression flakes group into islands uniformly distributed over the whole interface. With increasing surface pressure, the islands form a network which develops to a closed FLG film at the surface pressure of 38 mN/m (Fig.2.). At higher pressure the FLG film starts to collapse by overlapping of the FLG nanosheets. Above this pressure it is impossible to decompress the film to initial phases (islands or network) because of strong stitching of overlapped nanosheets.

After deposition the films were annealed up to 800 °C in the vacuum of 10⁻⁶ Pa. The resistance of the control samples was monitored in-situ using the Keithley source meter. Electrical contacts were made by silver paste compatible with vacuum ambient and temperature up to 930 °C glued to the film. Contacts were made 5 mm apart at the periphery of the substrate completely covered by the measured sample.

FLG nanofilms were decorated by the spin-coating of colloidal Pd NPs covered by oleylamine surfactant (6–7 nm, PlasmaChem, 0.1 mg/ml in chloroform). We prepared several samples with different concentrations of NPs by multiple spin-coating cycles with a constant drop volume of 5 μ l and rotation speeds of 10 or 75 rps. Scanning electron microscopy (SEM) analysis confirmed quite uniform distribution of NPs over the nanofilm surface with preferential location at the edges of flakes which are the chemically „hot“ sites [23]. Decoration was followed by 30 min vacuum heating at 350 °C to remove the surfactant, i.e. to guarantee the electrical contact between NPs and graphene. Decorated Pd NPs/FLG samples were studied by SEM. It was found that at high rotation speed of 75 rps Pd deposited density was low –

around 3 \times 10¹⁴/m² (Fig.3.a)) while at 10 rps it was medium – 3 \times 10¹⁵/m² (Fig.3.b)). This may be explained by the centrifugal force effect. Each additional spin-coating cycle at 10 rps increased the concentration of Pd NPs by 3 \times 10¹⁵/m². After 4 cycles the full coverage by NPs at the concentration of about 12 \times 10¹⁵/m² was obtained (Fig.3.c)). This density will be denoted as high.

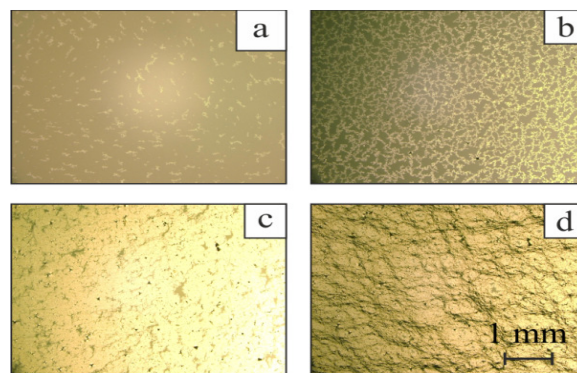


Fig.1. Successive phases of the FLG LS film formation at air/water interface: a) – islands, b) – network, c) – closed monolayer, d) – collapsed monolayer.

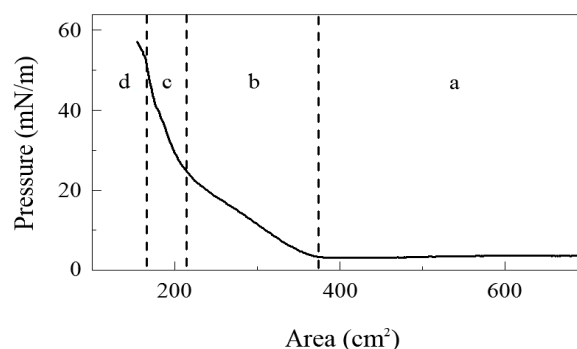


Fig.2. Surface-pressure isotherm in LS technique; a) – islands, b) – network, c) – closed monolayer, d) – collapsed monolayer, similarly as in Fig.1.

The pure and Pd NPs/FLG films were analyzed also by atomic force microscopy (AFM), X-ray diffraction (XRD), the Brunnauer-Emmett-Teller method (BET), and Raman spectroscopy. For the BET measurement volumetric apparatus (Polymer Institute of SAS) with Ar adsorbate at 77 K was used. Experimental gas sensors – chemiresistors were prepared by contacting the sensor medium with silver paste as above. The resistance response was studied at a constant voltage of 2 V in mixtures from 10 to 10 000 ppm of H₂ in dry air at 25, 50, and 70 °C and in mixtures from 2 to 6 ppm of NO₂ in dry air at 25, 100, and 200 °C. The sensor sensitivity was calculated as $\Delta R/R_a$, where ΔR is the change of resistance in the gas mixture vs. resistance R_a in air. Depending on the type of conductivity of the sensing medium sensitivity gets a negative or positive sign for oxidizing or reducing gases, respectively, as it will be shown. The gas concentrations were preset by dissolving the tested mixture in oxygen flow using precise mass flowmeters. The reference

FLG sample without Pd NPs was used in each measurement. During testing of sensors all R&D requirements on gas flow, mixture concentration, humidity and temperature were respected [20].

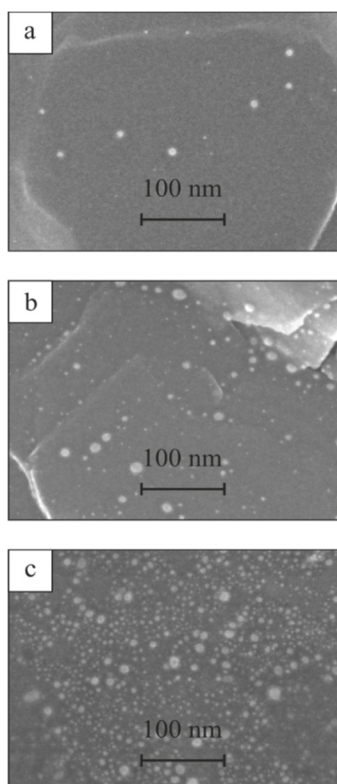


Fig.3. SEM images of FLG LS film decorated by Pd NPs with low a), medium b), and high c) densities obtained by spin-coating at 75 rps, 10 rps and 4 repeated cycles at 10 rps rotation speed, respectively.

3. RESULTS

The prepared FLG nanofilms are continuous with rare substrate naked areas covering about 0.1 % of the surface. An average FLG flake thickness and their lateral dimensions were estimated from AFM analysis as 5 nm and 300 nm, respectively [19].

The thickness equivalent to 10 – 15 graphene monolayers was estimated by Raman spectroscopy. Typical D, G, and 2D graphene bands were found at 1345 cm^{-1} , 1577 cm^{-1} , and 2692 cm^{-1} , respectively. From the lower intensity of D vs. G band relatively low density of defects in our samples is assumed. The intensity ratio $I_{2D}/I_G < 1$ corresponds to multilayered FLG deposit [19]. The XRD pattern of the FLG film (Fig.4.) exhibits a broad ripple suggesting a limited thickness of the FLG flakes restricted to few graphene monolayers. A shift of the ripple to smaller angles as compared to the principal 002 graphite diffraction indicates a swelling of the spacing between the monolayers from 0.337 nm in graphite to 0.404 nm in the FLG sample. From BET measurements it follows that the specific surface of our samples is from 8.5 up to 65.4 m^2/g . It is much lower than the theoretical value 2630 m^2/g of the monolayer completely exposed to the ambient. The dispersion of values depends on

the penetration of gas into the interlayer spaces. Another precondition of higher BET values is a careful drying of the samples.

In situ resistance of pure FLG nanofilm was measured in the vacuum of 10^{-6} Pa from RT up to 800 °C in a step-like mode (Fig.5.). At 300 °C the first irreversible drop of the resistance from 2 M Ω to 100 k Ω was recorded. After sequential increase of the temperature up to 800 °C the resistance dropped down to about 6 k Ω . The value of about 15 k Ω was achieved after cooling to RT. This way the samples were stabilized as confirmed by the repeated temperature cycling between RT and 800 °C. Also, the initial noise was suppressed. From RT resistance and contact geometry the resistivity of graphene deposit was estimated using calculations and $G(X,Y)$ function tabulated in [24]. Because of a two-contact measurement only an upper limit of 4300 $\mu\Omega\text{cm}$ was obtained. It can be compared with the resistivity of graphite 250 – 500 $\mu\Omega\text{cm}$ and $3 \times 10^5 \mu\Omega\text{cm}$ parallel and perpendicular to the basal plane, respectively.

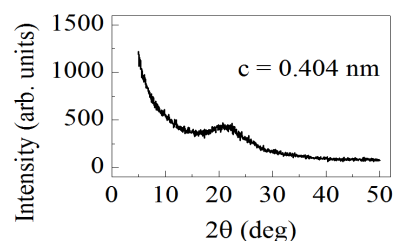


Fig.4. XRD pattern of FLG LS film.

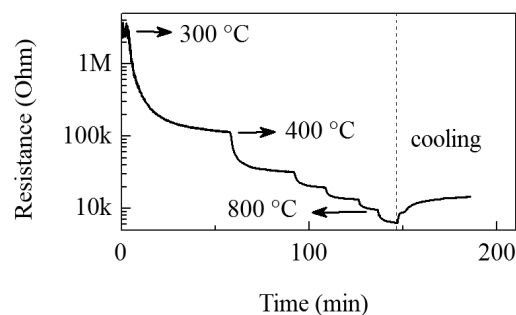


Fig.5. Time development of the electrical resistance of the FLG LS film on Si/SiO₂ substrate at the vacuum (10^{-6} Pa) heat treatment.

Our next step was the gas sensing measurement. During the exposure of FLG nanofilm to H₂ and NO₂ gases mixed in dry air the sensor resistance increased and decreased, respectively (Fig.6.a), Fig.6.b)). This is due to conduction electrons released from Pd-hydride at H₂ sensing (explained later) and, on the opposite, by capturing them by oxidizing NO₂ gas molecules (with high electron affinity of 2.28 eV as compared to 0.43 eV of oxygen) [25]. This points at the p-type conductivity of graphene. Let us mention that both p- and n-type of graphene are reported in the literature and even the change of the type of conductivity was observed (e.g., [26]).

Pure FLG film does not show any visible response to H_2 , but addition of Pd NPs changes the behavior dramatically (Fig.6.a)). Here the chemical reaction between Pd and hydrogen must be considered. When H_2 molecules get in touch with Pd NPs, they form palladium hydride PdH_x with a lower work function than that of pure Pd. This forces electrons from Pd atoms to the FLG film and increases the resistance of the whole system [27], [28]. The saturated response of 12 % was observed at high concentration of Pd NPs (Fig.6.c)) and even with 10 ppm of H_2 acceptable sensitivity of 4 % was recorded (Fig.7.a)).

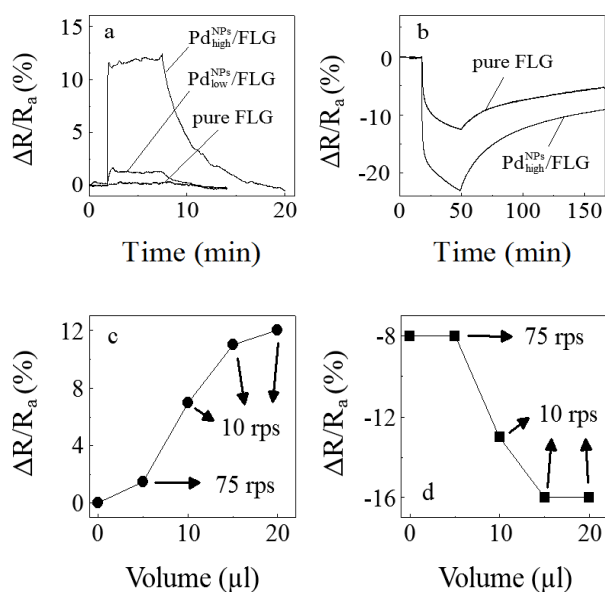


Fig.6. Gas response of Pd decorated FLG LS film and pure FLG LS reference sample to 10 000 ppm of H_2 gas a) and 6 ppm of NO_2 gas b) at RT. Effect of Pd NPs concentrations on gas response to 10 000 ppm of H_2 and 2 ppm of NO_2 at RT are shown in Fig.c) and Fig.d), respectively. Volume is the amount of Pd NPs solution applied onto the FLG nanofilm by spin-coating.

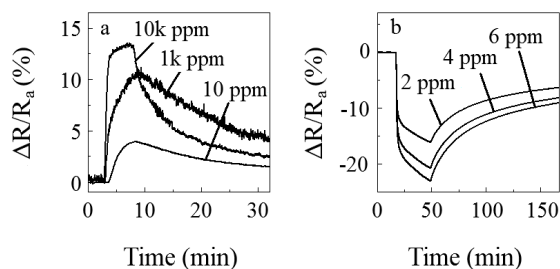


Fig.7. Sensitivity of Pd NPs decorated FLG LS film at different concentrations of H_2 a) and NO_2 b) at RT.

At higher temperatures the reaction accelerates and the response to 10 000 ppm of H_2 increases up to 26 % at 70 °C (Fig.8.a)). Moreover, the recovery of sensor is faster because also the decomposition of the PdH_x into hydroxyl and humidity is faster. Therefore, contrary to the NO_2 sensing, nitrogen flow was not effective to recover the H_2 gas sensor (Fig.9.a)).

Our sensors show a stable repeating cycle (Fig.10.a)). The baseline is growing only slightly. Response and recovery times are about 5 and 15 min, respectively.

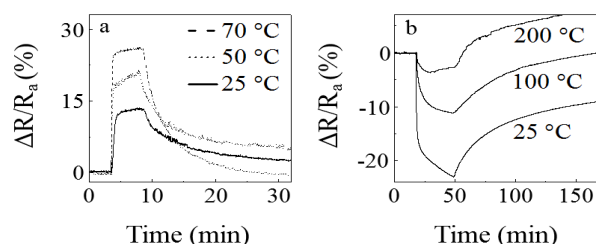


Fig.8. Gas response to 10 000 ppm of H_2 a) and 6 ppm of NO_2 b) at various working temperatures.

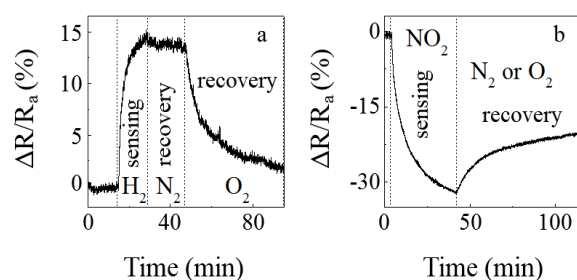


Fig.9. Recovery of the Pd NPs/FLG sensors after RT exposure to 10 000 ppm of H_2 a) and 200 ppm of NO_2 b).

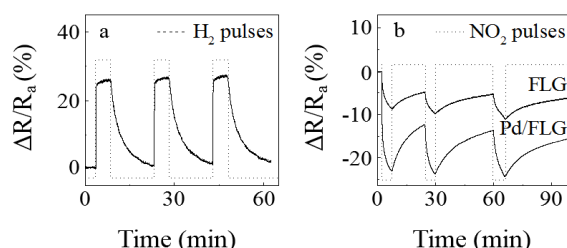


Fig.10. Dynamic response of the FLG sensor with high density of Pd NPs and of pure FLG reference sample at repeated exposures to 10 000 ppm of H_2 at 70 °C a) and 6 ppm of NO_2 at RT b) at the voltage of 2 V.

Pure FLG film sensors show certain response to NO_2 and by Pd decoration it is doubled to 23 % (Fig.6.b)). The saturated response to 2 ppm of NO_2 at high concentration of Pd NPs (Fig.6.d)) was 16 %. As expected, with growing NO_2 concentration the response increased (Fig.7.b)).

Higher operating temperatures accelerate the desorption of NO_2 from the surface of FLG flakes and the sensor response decreases (Fig.8.b)). Obviously, in this case, where only adsorption and desorption processes are involved, the sensor could be recovered either in nitrogen, oxygen or air (Fig.9.b)). Here the repeating cycle is less stable (Fig.10.b)) and it increases. The picture is similar for both pure FLG and Pd NP decorated samples, thus, the influence of Pd NPs might be excluded. The absorption of NO_2 molecules between the layers of multilayered FLG flakes might be an explanation. The response and full recovery times of our sensors are up to 40 min and 100 min, respectively, in this case.

The long-term stability of Pd decorated sensor response to NO₂ in air was studied as well. After 6 months the sensor signal decreased by 15 – 20 %. The decrease of sensitivity might be attributed to the oxidation of Pd NPs.

4. DISCUSSION

Many types of graphene materials are used nowadays for gas sensor preparation. Among them the FLG graphene could be prepared in a simple way, in sufficient quantities and without any complications with contacts formation. On the other hand, its properties differ from single layers or bilayers of graphene or very thin samples prepared either by micromechanical cleavage [6] or by epitaxy [27]. FLG samples show certain level of noise before high temperature stabilization, which can be attributed to the structural defects. Their concentration is not too large regarding the Raman spectra [19], nevertheless, it should be higher in material prepared by ultrasound disproportionation than in the case of mechanical cleavage. The annealing of defects is documented by the irreversible decrease of the sample resistance. Especially 1/f noise depends on the density of crystal defects [2].

Decoration of gas sensors by Pd or Pt is a standard approach to improve the sensor sensitivity or selectivity used for many years with metal oxides [29], [30] and recently also with graphene [5], [9], [10]. Among the mechanisms of improving the sensitivity of sensors by metallic additives the most frequent are: a) electronic effects, b) enhancement of gas adsorption combined with spillover effect, c) catalytic increase of the rate of reaction of gas on the sensor surface, d) growth of the adsorption on the surface by coarsening/roughening process. Having in mind the lower effectivity of low density Pd coverage for increasing the sensor response to NO₂ gas (Fig.6.d) the mechanism b) (spillover effect) is less probable. The decrease of the sensor response with increasing temperature favors mechanism d). It should be mentioned that with graphene sensors of hydrogen decorated by Pd and Pt ([5] and [9], respectively), electronic mechanisms are assumed, similarly as in the case of Pd decorated graphene for NH₃ monitoring [10], where the response was also improved. However, with the same sensor the response to NO₂ due to Pd presence was smaller. In our H₂ sensing we favor the mechanism of palladium hydride formation. But Pd influence upon gas sensing is a complex one and electronic mechanism of the Pd action must be considered also in our case.

We should admit also that the sensor response expressed as a ratio of currents measured with and without the monitored gas of our, but also other graphene sensors, is lower than in the case of metal oxides with high resistance. There, the smaller currents are more influenced by gas adsorption. In more conductive graphene sensors these changes are smaller. Nevertheless, both types of devices are comparable in terms of sensitivity being in the ppm – ppb range [31]. The mutual sensitivities of our sensors to H₂ and NO₂ in this paper cannot be compared because of different mechanisms of sensing.

Finally, let us mention that the BET specific surface areas of graphene samples prepared by various methods differ

considerably and they are much lower than the theoretical maximum of 2 630 m²/g. Some typical data between 300 and 1 000 m²/g are reported in [32]. This is because as-prepared graphene easily agglomerates due to the large surface area and surface energy. With graphene for lithium-ion batteries obtained by exfoliation of graphene oxide and consisting of 4-layer sheets the surface area was 492.5 m²/g, [33]. In our case the graphene flakes are thicker, about 10–15 monolayers, and that may be the reason of lower surface area values measured here. The structure composed of flakes with boundaries between them explains the measured resistivity of the material which is of the same order of magnitude as the resistivity of graphite.

5. CONCLUSIONS

The FLG sensors decorated by Pd NPs proved to be sufficiently sensitive to both H₂ and NO₂ gases at the concentration of 10 000 ppm and 6 ppm in dry air, respectively, even at RT. The application of sensors at RT is a considerable advantage of graphene vs. metal oxide devices. The mentioned sensitivities are of practical interest in hydrogen energy management or in environment protection. The upper limit of Pd NP density corresponding to the saturation of sensor response was determined. A big advantage of graphene is its excellent stability due to strong sp² bonds. However, the decoration with reactive metals, like palladium, may be a reason for the slow long-term drift of sensor properties. The defect density of as-deposited FLG could be suppressed by annealing, thus decreasing the electrical resistance and also initial noise level. The high-frequency measurement might be applied in further studies to explain the electrical conductivity of FLG films composed of flakes. The relatively slow sensor recovery at the NO₂ sensing may be caused by the penetration of gas molecules into the inter-flake spaces. Faster recovery at the H₂ detection is due to different mechanisms of sensing based upon the Pd surface chemical reactions. Because of high graphene conductivity the sensor response expressed as a ratio of currents measured with and without the monitored gas is smaller as compared to metal oxide devices. But in terms of low detection limit both types of sensors are comparable.

ACKNOWLEDGEMENT

The work was supported by grants of the Slovak Research and Development Agency 14-0891 and 15-0641 and by grant agency VEGA Bratislava, project No. 2/0081/18. The help with BET measurement by Dr. I. Novak (Polymer Inst. SAS) is acknowledged.

REFERENCES

- [1] Seiyama, T., Kato, A., Fujiishi, K., Nagatani, M. (1962). A new detector for gaseous components using semiconductive thin films. *Analytical Chemistry*, 34, 1502-1503.
- [2] Basu, S., Bhattacharyya, P. (2012). Recent developments on graphene and graphene oxide based solid state gas sensors. *Sensors and Actuators B*, 173, 1-21.

- [3] Llobet, E. (2013). Gas sensors using carbon nanomaterials: A review. *Sensors and Actuators B*, 179, 32-45.
- [4] Varghese, S. S., Lonkar, S., Singh K. K., Swaminathan, S., Abdala, A. (2015). Recent advances in graphene based gas sensors. *Sensors and Actuators B*, 218, 160-183.
- [5] Wang, T., Huang, D., Yang Z. et al. (2016). A review on graphene-based gas/vapor sensors with unique properties and potential applications. *Nano-Micro Letters*, 8 (2), 95-119.
- [6] Yang, S., Jiang, C., Wei, S.-H. (2017). Gas sensing in 2D materials. *Applied Physics Reviews*, 4, 021304.
- [7] Huo, N., Yang, S., Wei, Z. et al. (2014). Photoresponsive and gas sensing FET based on multilayer WS₂ flakes. *Scientific Reports*, 4, 5209-5221.
- [8] Li, H., Wu, J., Yin, Z., Zhang, H. (2014). Preparation and applications of mechanically exfoliated single-layer and multilayer MoS₂ and WSe₂ nanosheets. *Accounts of Chemical Research*, 47, 1067-1075.
- [9] Cagliani, A., Mackenzie, D., Tschammer, L.K., Pizzocchero, F., Almdal, K., Bøggild, P. (2014). Large-area nanopatterned graphene for ultrasensitive gas sensing. *Nano Research*, 7 (5), 743-754.
- [10] Chung, M.G., Kim, D.-H., Seo, D.K. et al. (2012). Flexible hydrogen sensors using graphene with palladium nanoparticle decoration. *Sensors and Actuators B*, 169, 387-392.
- [11] Chu, B.H., Lo, C.F., Nicolosi, J. et al. (2011). Hydrogen detection using platinum coated graphene grown on SiC. *Sensors and Actuators B*, 157, 500-503.
- [12] Cho, B., Yoon, J., Hahm, M.G. et al. (2014). Graphene-based gas sensor: Metal decoration effect and application to a flexible devices. *Journal of Materials Chemistry C*, 2, 5280-5285.
- [13] Chung, M.G., Kim, D.H., Lee, H.M. et al. (2012). Highly sensitive NO₂ gas sensor based on ozone treated graphene. *Sensors and Actuators B*, 166-167, 172-176.
- [14] Schedin, F., Geim, A.K., Morozov, S.V. et al. (2007). Detection of individual gas molecules adsorbed on graphene. *Nature Materials*, 6 (9), 652-655.
- [15] Hernandez, Y., Nicolosi, V., Lotya, M. et al. (2008). High-yield production of graphene by liquid-phase exfoliation of graphite. *Nature Nanotechnology*, 3, 563-568.
- [16] Nemade, K.R., Waghuley, S.A. (2013). Chemiresistive gas sensing by few-layered graphene. *Journal of Electronic Materials*, 42, 2857-2866.
- [17] Kim, H.K., Mattevi, C., Kim, H.J. et al. (2013). Optoelectronic properties of graphene thin films deposited by Langmuir-Blodgett assembly. *Nanoscale*, 5, 12365-12374.
- [18] Ko, G., Kim, H.-Y., Ahn, J., Park, Y.M., Lee, K.-Y., Kim, J. (2010). Graphene based nitrogen dioxide gas sensors. *Current Applied Physics*, 10, 1002-1004.
- [19] Kostiuk, D., Luby, S., Demydenko, M. et al. (2016). Few-layer graphene Langmuir-Schaefer nanofilms for H₂ gas sensing. *Procedia Engineering*, 168, 243-246.
- [20] Capone, S., Benkovicova, M., Forleo, A. et al. (2017). Palladium/ γ -Fe₂O₃ nanoparticle mixtures for acetone and NO₂ gas sensors. *Sensors and Actuators B*, 243, 895-903.
- [21] Jia, W., Tchoudakov, R., Narkis, M., Siegmann, A. (2005). Performance of expanded graphite and expanded milled graphite fillers in thermosetting resins. *Polymer Composites*, 26 (4), 526-533.
- [22] Chitu, L., Siffalovic, P., Majkova, E., Jergel, M., Luby, S. (2014). *Method of the preparation of nanoparticle monolayers and multilayers*. Slovak patent No. 288234. Bratislava: The Industrial Property Office of SR. (in Slovak)
- [23] Hoffmann, R. (2013). Small but strong lessons from chemistry for nanoscience. *Angewandte Chemie*, 52, 93-103.
- [24] Hall, P.M. (1997). Resistance calculations for thin film rectangles. *Thin Solid Films*, 300, 256-264.
- [25] Afzal, A., Cioffi, N., Sabbatini, L., Torsi, L. (2012). NO_x sensors based on semiconducting metal oxide nanostructures: Progress and perspectives. *Sensors and Actuators B*, 171-172, 25-42.
- [26] Pearce, R., Iakimov, T., Andersson, M., Hultman, L., Lloyd Spetz, A., Yakimova, R. (2011). Epitaxially grown graphene based gas sensors for ultra sensitive NO₂ detection. *Sensors and Actuators B*, 155, 451-455.
- [27] Phan, D.-T., Chung, G.-S. (2014). A novel Pd nanocube-graphene hydride for hydrogen detection. *Sensors and Actuators B*, 199, 354-360.
- [28] Yi, J., Kim, S.H., Lee, W.W. et al. (2015). Graphene meshes decorated with paladium nanoparticles for hydrogen detection. *Journal of Physics D: Applied Physics*, 48, 475103.
- [29] Ménini, P., Parret, F., Guerrero, M. et al. (2004). CO response of a nanostructured SnO₂ gas sensor doped with palladium and platinum. *Sensors and Actuators B*, 103, 111-114.
- [30] Biswal, R.C. (2011). Pure and Pt-loaded γ -iron oxide as sensor for detection of sub ppm level of acetone. *Sensors and Actuators B*, 157, 183-188.
- [31] Wetchakun, K., Samerjai, T., Tamaekong, N. et al. (2011). Semiconducting metal oxides as sensors for environmentally hazardous gases. *Sensors and Actuators B*, 160, 580-591.
- [32] Dai, J.-F., Wang, G.-J., Ma, L., Wu, C.-K. (2015). Surface properties of graphene: Relationship to graphene-polymer composites. *Reviews on Advanced Materials Science*, 40, 60-71.
- [33] Lian, P., Zhu, X., Liang, S. et al. (2010) Large reversible capacity of high quality graphene sheets as an anode material for lithium-ion batteries. *Electrochimica Acta*, 55, 3909-3914.

Received January 28, 2019

Accepted April 12, 2019